

Application of Langmuir-Hinshelwood Model to Bioregeneration of Activated Carbon Contaminated With Hydrocarbons

¹Ameh, C.U., ²Jimoh, A., ³Abdulkareem, A.S. and ⁴Otaru, A.J.

¹(Chevron Nigeria Limited, 2, Chevron Drive, Lekki, Lagos, Nigeria).

^{2,3&4}(Department of Chemical Engineering, Federal University of Technology, Minna, Nigeria)

Abstract: Environmental pollution, high cost and high energy consumption associated with thermal regeneration of activated carbon polluted with hydrocarbon necessitated the search for a better way of regenerating activated carbon, bioregeneration. Spent granular activated carbon was regenerated having been initially characterized using cultured *Pseudomonas Putida*. The rate of bioregeneration was studied by varying the volume of bacteria from 10ml, 20ml, 30ml and 40ml. The regeneration temperature was also varied from 25°C to ambient temperature of 27°C, 35°C and further at 40 and 45°C over a period of 21 days. The experimental results showed clear correlation when validated using the Langmuir-Hinshelwood kinetic model. The experiment at ambient temperature showed a negative correlation due to the fluctuation in the ambient temperature unlike all other experiment where temperature was controlled in an autoclave machine.

Keywords: Bioregeneration, GAC, Model, Nigeria and Pollution.

I. Introduction

Nigeria, like any other developing countries has engaged in extensive oil exploration activities (being the major source of revenue) to stimulate her economic growth since the discovery of crude oil about 55 years ago (Nwankwo and Ifeadi, 1988). The dependence of the nation on crude oil exploitation has been attributed to the degree of economic benefits that can be derived and subsequently channelled towards development, growth and sustainability (Sanusi, 2010). For instance, as at 1976, oil export was reported to have accounted for about 14% of the Gross Domestic Product (GDP), 95% of total export (Nwankwo and Ifeadi, 1988) and about 80% of government annual revenue (Nwankwo and Ifeadi, 1988). The trend remains the same even though crude oil is a non-renewable source of wealth that may vanish with time. All attempts by government to diversify the economy and reduce over dependency on oil exploitation as major source of revenue ends up as rhetoric, which implies that oil is still the mainstay of the Nigerian economy (Sanusi, 2010).

Production and consumption of oil and petroleum products are increasing worldwide, and the risk of oil pollution is increasing accordingly. The movement of petroleum from the oil polluted site is still rising. The movement of petroleum from the oil fields to the consumer involves as many as 10 to 15 transfers between many different modes of transportation, including tanks, pipelines, railcars, and trucks (Fingas, 2011). Accidents can occur during any of these transportation steps or storage times. An important part of protecting the environment is ensuring that there are as few spills as possible. Both government and industry in developed countries are working to reduce the risk of oil spills by introducing strict new legislation and stringent operating codes. In Nigeria, the much dependence on the exploration of crude petroleum has hampered the implementation of her decree. The low penalty cost even encouraged the abrogation of the decree by the companies (Ayaegbunami, 1998). As human and environment respond to environmental pollution, the environmental engineer faces the rather daunting task of elucidating evidence relating cause and effects. This calls the attention to finding a better way of remediating petroleum polluted site using adsorbent and of economic benefit, regeneration of used adsorbent.

Adsorbent like activated carbon (AC) have the capacity to remove contaminants up to an allowable concentration and subsequently loses its sorption capacity after been saturated (Amer and Hussein, 2006). It is important to regenerate such AC so as to regain most of its sorption capacity and be available for reuse. This became necessary due to the expensive nature of most of the commercial available AC in use (Amer and Hussein, 2006). Thermal regeneration which is another option actually consumes money and energy as the temperature of reactivation alone is about 600 – 900°C (Bagreev *et al*, 2000). Carbon losses (Moreno-Castilla, 1995) will be present too due to burnout when using heat to regenerate. There is also the issue of environmental pollution inherent in the use of thermal regeneration (Dehdashti, 2010).

Efficiency, cost and convenience are of major importance. Mathematical model presents a realistic way of addressing experimental results. Mathematical models can provide valuable information to analyze and predict the performance of bioregeneration of activated carbon. It is important to gain an understanding of operations where time-variant influent concentrations and multiple substrates are encountered (Speitel *et al.*, 1987). The bioregeneration model requires the mathematical description of two distinct processes (Speitel *et al.*,

1987), the kinetics of adsorption/desorption in the activated carbon column and kinetics of microbial growth and solute degradation in the activation column. This research therefore looks into the application of Langmuir-Hinshelwood equation on an experiment results on bioregeneration of activated carbon contaminated with hydrocarbon. The Langmuir-Hinshelwood model is established from Monod equation.

II. Research methodology

Extracted used activated carbon was treated with pseudomonas putida bacteria culture. This treatment take place in a Bioreactor set up in a laboratory. The rate of hydrocarbon degeneration was measured at intervals of 24 hours for 21 days by collecting samples and testing for hydrocarbon content and concentration. Evidence of activated carbon regeneration occurred due to the reduction in total hydrocarbon content in the sample over the 21 days. These values were validated using the Langmuir- Hinshelwood equation (Kumar *et al*, 2008) established from Monod equation. Also, comparison between the experimental results and modelled results were correlated using the correlation coefficient function in Microsoft Excel.

III. Working Model

Kinetics of Microbial Growth and Solute Degradation

The performance of the Biological Activated Carbon system is a simple combination of adsorption and biodegradation. Bio-film development is described by the Monod model leading to substrate utilization increasing exponentially. Eventually, the thickness of the active bio-film becomes limited by substrate penetration, oxygen penetration or hydrodynamic shear, and it is assumed that the rate of substrate utilization becomes constant at its maximum value (Walker & Weatherley, 1997). The growth of microorganisms can be modelled by Monod equation.

$$\mu = \frac{\mu_{max} S}{K_S + S} \quad (1)$$

Where μ is the specific growth rate, μ_m is the maximum specific growth rate, K_s is the half saturation coefficient and S is the substrate concentration.

The pathways of substrates after entering the bio-film are biodegradation and metabolism-dependent processes such as bio-sorption (Aksu and Tunc, 2005). Similar type of equation was proposed by Lin and Leu (2008) to describe the simultaneous adsorptive decolourization and degradation of azo-dye by *Pseudomonas luteola* in a biological activated carbon process. Goeddertz *et al.*, (1988) used Haldane type biodegradation kinetics to model the bioregeneration of granular activated carbon saturated with phenol. The rate of biodegradation, r_1 , for an inhibitory substance can be modelled using Haldane expression:

$$r_1 = -\left(\frac{\mu}{Y}\right) \quad (2)$$

$$\mu = \frac{\mu_{max} C}{K_S + C + \left(\frac{C^2}{K_i}\right)} \quad (3)$$

Where, X is the biomass concentration, Y yield coefficient and K_s , K_i are the Haldane constants. The model successfully predicted the bulk liquid substrate concentrations when phenol was the substrate, as well as the extent of bioregeneration.

Langmuir-Hinshelwood model

Just as the term Michelis-Mentin kinetics is used to describe the kinetics of enzyme-catalyzed reactions that follow one simple type of reaction mechanism, the term Langmuir Hinshelwood kinetics generally refers to heterogeneous catalytic reaction kinetics that can be described by a simple mechanistic model. In Langmuir-Hinshelwood models, the surface of the catalyst is modeled as being energetically uniform, and it is assumed that there is no energetic interaction between species adsorbed on the surface. These are the same assumptions that Langmuir used in deriving his isotherm to model surface adsorption processes. Each reactant is assumed to adsorb on a surface site. Following surface reaction between adsorbed reactants to generate surface products, the products desorbed from the surface.

Model equation for validating experimental results

Regeneration usually involves the adsorbed contaminants from the activated carbon using temperatures or processes that drive the contaminants from the activated carbon but do not destroy the contaminants or the activated carbon. The growth of microorganisms can well be explained by Langmuir – Hinshelwood equation which can be formulated from Monod equation as in equation (1).

$$\mu = \frac{\mu_{max} S}{K_S + S}$$

Where μ is the specific growth rate, μ_m is the maximum specific growth rate, K_s is the half saturation coefficient and S is the substrate concentration.

$$\mu = \frac{\mu_{max} S}{K_S + S}$$

$$\mu = \frac{\mu_{max} \cdot S}{K_S \left(\frac{K_S}{K_S} + \frac{1}{K_S} \cdot S \right)}$$

$$\mu = \frac{\mu_{max} / K_S \cdot S}{\left(1 + \frac{1}{K_S} \cdot S \right)}$$

Let $K^* = \mu_{max} / K_S$, $C_A = S$, and $K_A = \frac{1}{K_S}$

Hence,

$$r_{A=} = \frac{K^* C_A}{1 + k_A C_A} \quad \text{(Langmuir-Hinshelwood equation)} \quad (4)$$

Where $r_{A=}$ adsorption rate (g/hr), C_A is the adsorbed concentration (grams), the constant K^* and k_A are equilibrium constants and can be best obtained using the least mean square method (LMSM) presented below.

Least Mean Square Method (LMSM)

Using the formulated Langmuir Hinshelwood equation

$$r_{A=} = \frac{K^* C_A}{1 + k_A C_A}$$

$$\text{let } R = \frac{1 + k_A C_A}{K^*} = \frac{1}{K^*} + \frac{k_A}{K^*} C_A$$

$$\text{let } a = \frac{1}{K^*} \text{ and } b = \frac{k_A}{K^*}$$

$$R = a + b C_A \text{ and } r_{A=} = \frac{C_A}{R}$$

$$R = \frac{C_A}{r_{A=}} = a + b C_A \quad (5)$$

Since $R = a + b C_A$ is a linear equation, a and b can be determined by method of LMSM (least mean square method).

To find a we multiply equation (5) by the coefficient variable of a and taking the summation of both LHS and RHS of the equation.

$$\sum (1) R = \sum (1) \cdot a + \sum (1) C_A$$

$$\frac{\sum R - b \sum C_A = a}{n} \quad (6)$$

To find b we multiply equation (5) by the coefficient variable of b (i.e. C_A) and take the summation sign.

$$\sum R C_A = \sum a C_A + \sum b C_A^2$$

$$\sum R \cdot C_A = a \sum C_A + \sum b C_A^2 = \left(\frac{\sum R - b \sum C_A}{n} \right) \sum C_A + b \sum C_A^2$$

$$\sum R \cdot C_A = \left(\frac{\sum R \cdot \sum C_A - b(\sum C_A)^2}{n} \right) + b \sum C_A^2$$

$$n \cdot (\sum R) \cdot C_A = \sum R \cdot \sum C_A - b(\sum C_A)^2 - b \cdot n \cdot \sum C_A^2$$

$$n \cdot \sum R \cdot C_A - \sum R \cdot \sum C_A = b[n \cdot \sum C_A^2 - (\sum C_A)^2]$$

$$b = \frac{n \cdot \sum R \cdot C_A - \sum R \cdot \sum C_A}{n \cdot \sum C_A^2 - (\sum C_A)^2}$$

$$b = \frac{\sum R \cdot C_A - \sum R \cdot \sum C_A / n}{\sum C_A^2 - (\sum C_A)^2 / n} \tag{7}$$

In summary

$$R = a + bC_A$$

$$r_A = \frac{C_A}{R} \text{ as } R = \frac{C_A}{r_A}$$

$$a = (\sum R - b \sum C_A) / n$$

$$b = \frac{\sum R \cdot C_A - \sum R \cdot \sum C_A / n}{\sum C_A^2 - (\sum C_A)^2 / n}$$

$$a = \frac{1}{K^*} = K^* = \frac{1}{a}$$

$$b = \frac{K_A}{K^*}$$

$$r_A = \frac{K^* C_A}{1 + K_A C_A}$$

The adsorption rate r_A is defined mathematically above. Also, comparison between the experimental results and modelled results were correlated using the correlation coefficient function in Microsoft Excel.

IV Results and Discussions

Figure 1 compared the adsorption rates obtained using experimental parameters and that simulated using Langmuir-Hinshelwood equation when 10 ml volume of bacteria was used to treat used GAC. It can be seen that both curves plotted against time (t) depict the behaviour indicating decrease in adsorption rate with time for the first few days, followed by an almost constant adsorption rate for most of the experimental duration. The curves show an increase in the rate of adsorption towards the end of the experiment.

The value of correlation coefficient for both set of data was calculated as **0.78** for the entire experiment duration. However, when the set of data was considered from the 1st day of the experiment to the 18th day, the correlation coefficient significantly improved to **0.97** which shows that there is a very good agreement between experimental results obtained in the current study and the simulated results obtained using Langmuir-Hinshelwood equation for the first 18 days of the experiment..

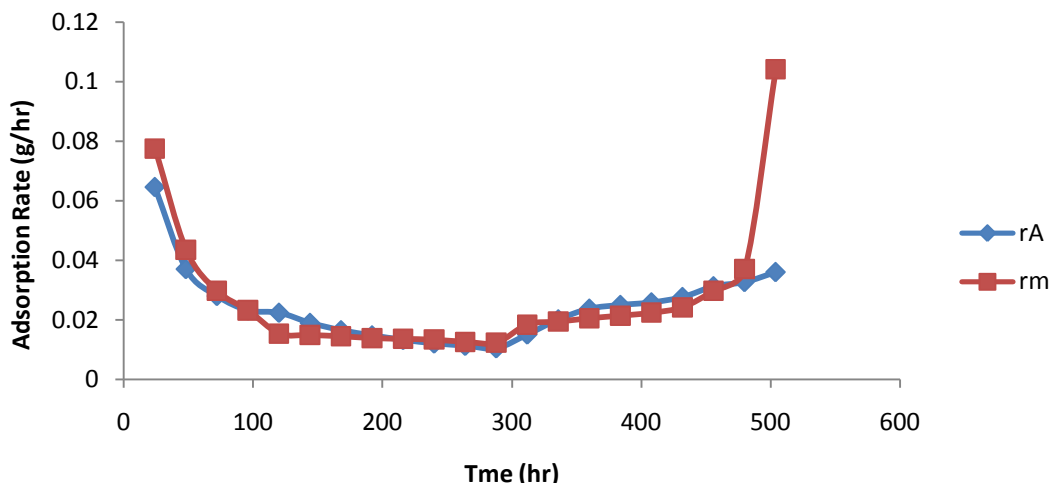


Figure 1: Validation of experimental result for 10ml bacteria

Using the Langmuir-Hinshelwood equation (Kumar *et al*, 2008), simulation results obtained for adsorption rates were compared with adsorption rates calculated from experimental results obtained for GAC treated with 20 ml bacteria. The graphical behaviour of both set of data is as presented in Figure 2. The correlation coefficient was determined using Microsoft Excel program to be **0.35** when the entire experimental results for the 21 days were considered. However, considering the experimental result and the modelled result for the initial 18 days also, the correlation coefficient significantly improved to **0.81**.

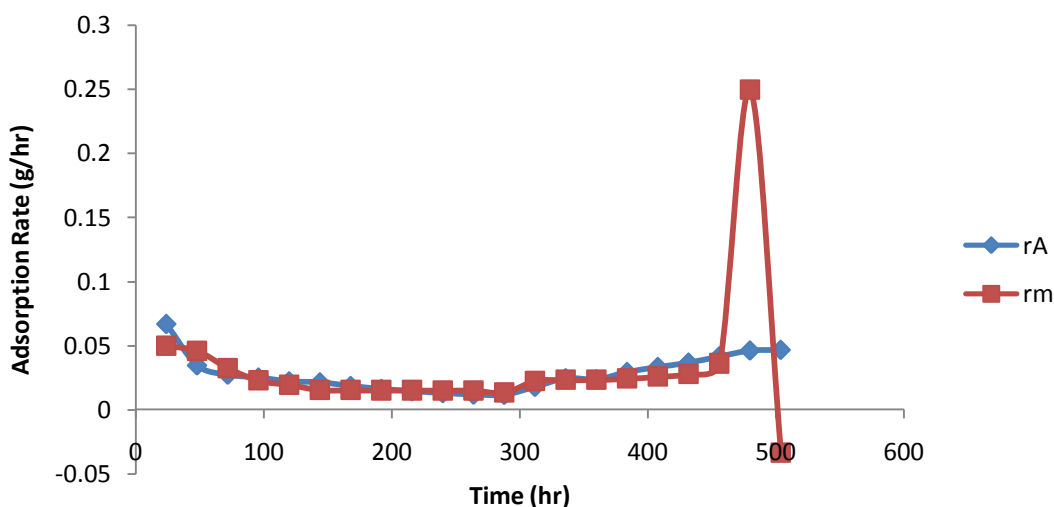


Figure 2: Validation of Result for 20ml bacteria

The simulation results obtained for adsorption rates were also compared with adsorption rates calculated from experimental results obtained for GAC treated with 30 ml bacteria. The graphical behaviour of both set of data is as presented in Figure 3. The correlation coefficient was determined using Microsoft Excel program to be **0.07** when the result for the entire 21 days was considered. However, just like in the 10 and 20ml experimental result validation, the correlation when the initial 18 days was considered was **0.98** giving an almost perfect fit.

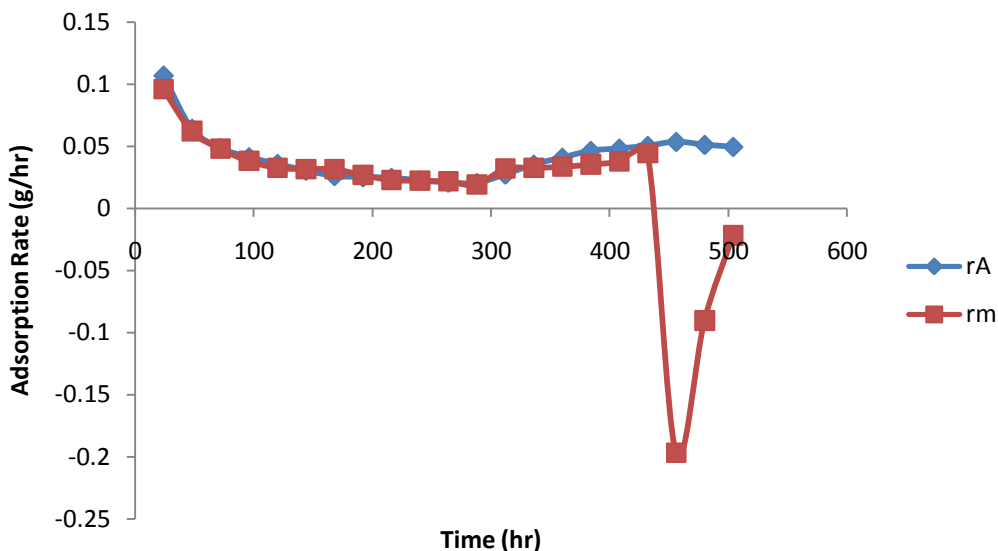


Figure 3: Validation of Result for 30ml bacteria

Figure 4 also shows the plot for the validation of the experimental result against the modelled result for the experiment using 40ml bacteria volume. The correlation coefficient for the entire 21 days experimental results gave **0.17** but when the initial 18 days results were considered; the correlation coefficient significantly improved giving a near perfect fit of **0.98**.

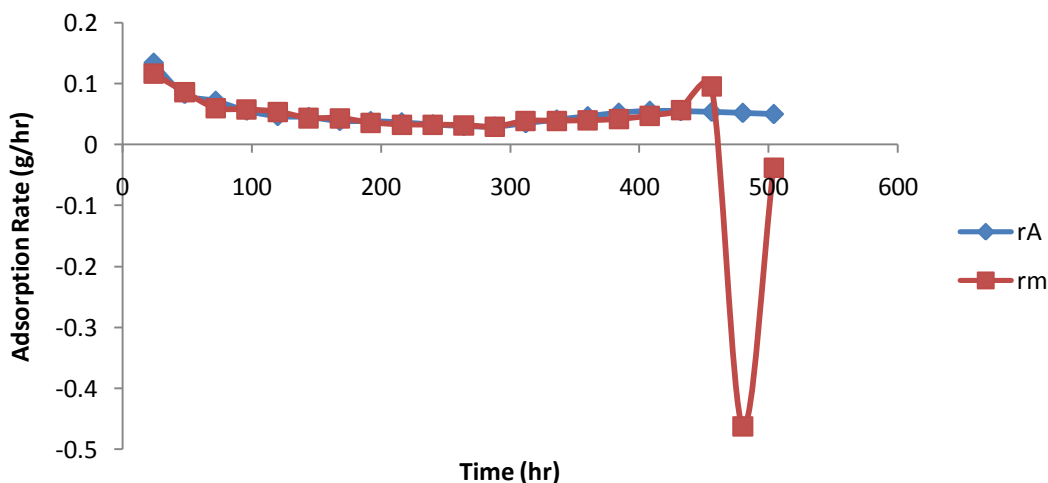


Figure 4: Validation of Result for 40ml bacteria

Taking a critical look at the graphs on Figures 1, 2, 3 and 4, the behaviour indicates the same phenomenon and the adsorption rate can be seen to reduce gradually for the first few days only to stabilise for most of the experiment period. It is important to note that the curves are similar and that the correlation for both results for the four graphs indicates a perfect fit until the 19th day of the experiment. Irrespective of the increase in bacteria volume, this behaviour remains the same for all the samples.

Figure 5 shows the plot for the validation of the experimental result for the experiment at 25°C. This experiment was conducted below the prevailing atmospheric temperature of 27°C at the time of the experiment. The plot indicates a degree of correlation with the coefficient of **0.65** when the entire experimental result was compared with the modelled result. The coefficient of correlation increased however to **0.69** when considered from the 3rd to the 21st day.

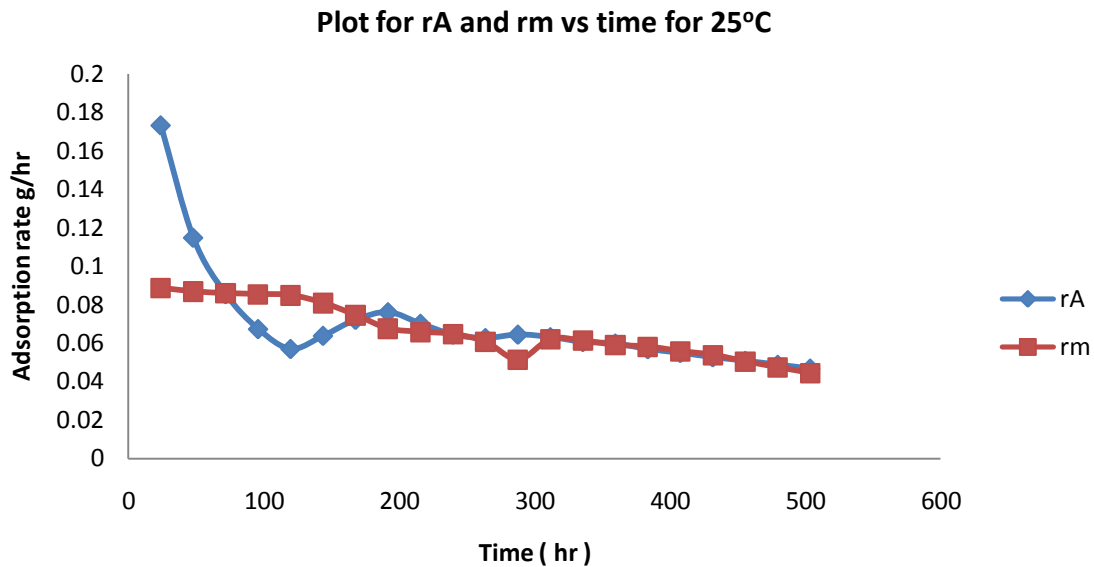


Figure 5 Validation of Result for 25°C temperature

Figure 5 shows the plot for the experimental result against the simulated results using the Langmuir-Hinshelwood kinetic equation (Kumar *et al.*, 2008) for the experiment at atmospheric temperature of 27°C. The plot showed a negative correlation of **-0.06** when the entire experimental duration was considered. However, the experimental result and the modelled result showed a good fit of **0.85** when the results from the 1st day to the 16th day was considered. This is attributed to the impact of atmospheric temperature variation.

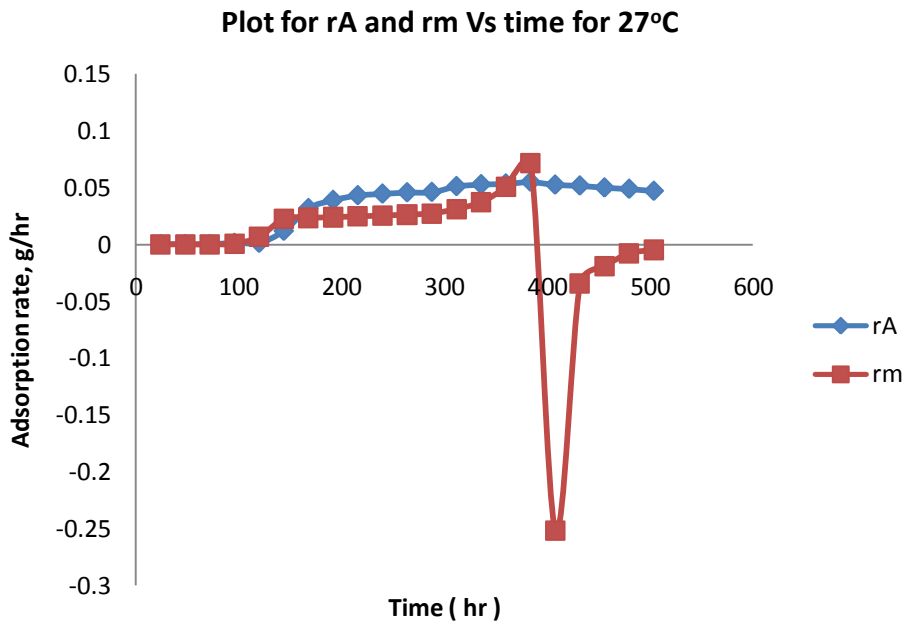


Figure 5 Validation of Result for 27°C temperature

Figure 6 shows the plot for the experimental result at 35°C against the result obtained using the kinetic model used in the prior validations above. The correlation between the modelled and experimental result for the entire experiment duration gave a poor fit of **0.33**. When the results from the 3rd day to the 21st day was considered also, there was a poor fit of **0.35**.

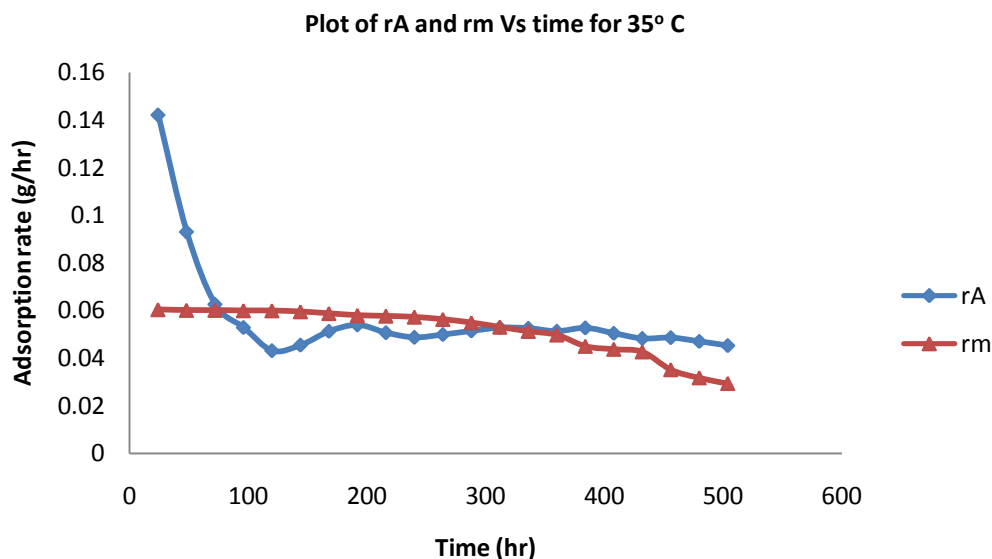


Fig 6: Validation of Result for 35°C temperature

Figure 7 shows the plot for the experimental result at 40°C against the result obtained using the kinetic model used in the prior validations as above. . The correlation between both results for the entire experiment duration gave a negative fit of **-0.6**. When the results from the 2nd day to the 21st day were considered, there was a poor fit of **-0.3**.

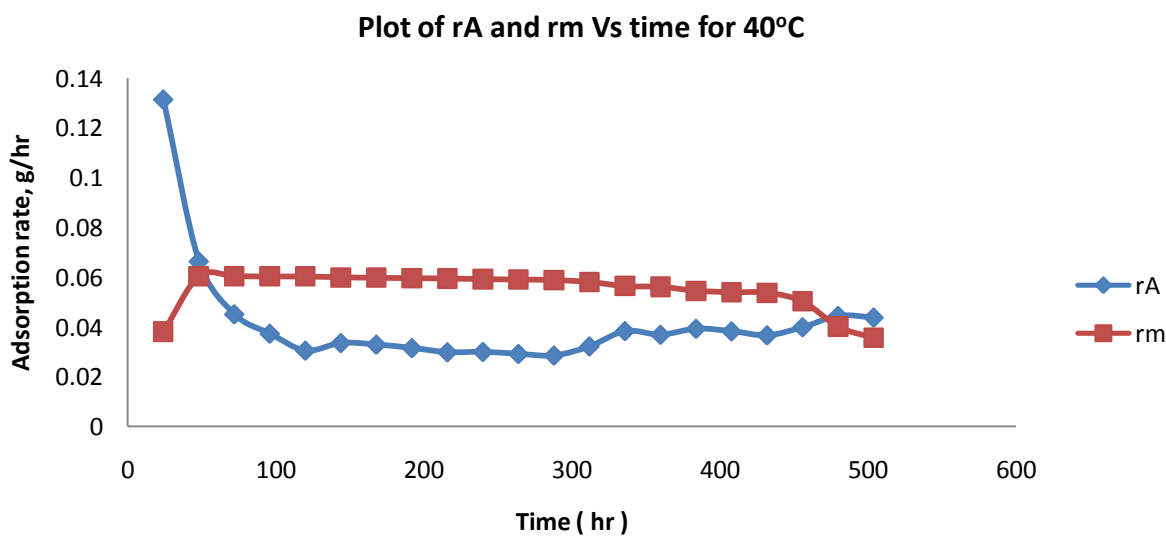


Figure 7 Validation of Result for 40°C temperature

Figure 8 shows the plot for the experimental result at 45°C against the result obtained using the kinetic model used in the prior validations. The correlation between both results for the entire experiment duration gave an excellent fit of **0.93**. When the entire results from the 1st day to the 21st day was considered. There was even a better fit of **0.98** when the results from the 1st to the 20th day was considered.

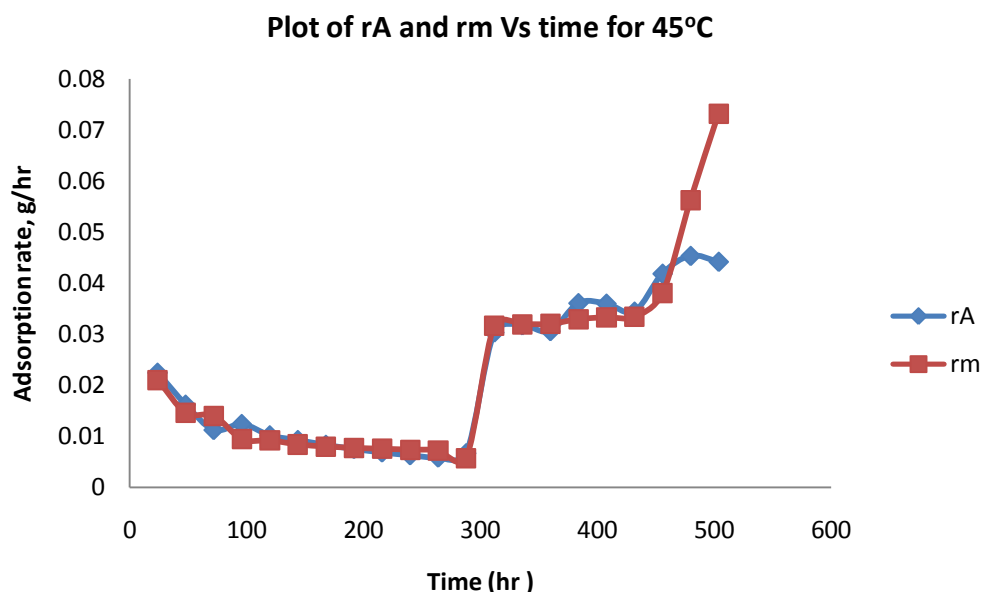


Figure 8: Validation of Result for 45°C temperature

Taking a look at the regeneration efficiency for the temperatures of 25, 27, 35, 40 and 45°C as considered above, results obtain were 96.8, 97.4, 93.7, 90.8 and 91.5% respectively. This clearly showed that the experiment at 27°C which was the room temperature was the most efficient regeneration temperature. It implies that the bioregeneration efficiency did not improve with increase in temperature above the room temperature (Delage, 1999).

V. Conclusions

Bioregeneration is very effective in recovering spent granulated activated carbon (GAC) for reuse considering the quality of the regenerated GAC in comparison to a virgin sample. Temperature plays an important role in bioregeneration efficiency and increasing the temperature improved the efficiency in as much as it is beyond the temperature that will incapacitate the bacteria colony. Effective bioregeneration was achieved at 40°C as such it is concluded that increasing the temperature of bioregeneration to 45°C was not cost effective. Also, increasing the volume of bacteria increased the rate of bioregeneration. The validation of the experimental result also leads to the conclusion that there is clear correlation between the experimental results and the Langmuir-Hinshelwood kinetic model.

Acknowledgements

I wish to express my appreciation to Mr. OTARU, Abdulrazak and all my course mates of the 2010/11 M.Eng students in the Department of Chemical Engineering, Federal University of Technology Minna, Nigeria for the support and comradeship while the program lasted.

References

- [1]. Aksu, Z. and Tunc, O (2005): Application of biosorption for penicillin G removal: comparison with activated carbon. *Process Biochemistry*. Vol 40 (2):831–847.
- [2]. Amer, A.A. and Hussein, M. (2006): Bagasse as oil spill cleanup sorbent 2. Heavy oil sorption using carbonized pith bagasse fibre.
- [3]. The second International Conference on Health, Environment and Development, ICHEDI, Alexandria, Egypt.
- [4]. Ayaegbunami, E. (1998). *Coping with Climate and Environmental Degradation in the Niger Delta*. CREDC.
- [5]. Dehdashti, A., Khavanin, A., Rezaee, A & Asilian, H (2010): Regeneration of Granular Activated Carbon Saturated with Gaseous Toluene by Microwave Irradiation. Published in the *Turkish Journal of Engineering and Environmental Science*. Volume 34. 2010. pp 49 - 58.
- [7]. Goeddertz, J.G., Weber, A.S., Matsumoto, M.R. (1988): Offline bio-regeneration of Granular Activated Carbon (GAC), *Journal of Environmental Engineering Science*, Vol 5, 114: 1063-1076.
- [8]. Fingas, M. (2011). *The Online Version of Oil Spill Science and Technology*. ScienceDirect.com
- [9]. Kumar, K. V., Porkodi, K and Rocha, F (2008): Langmuir-Hinshelwood Kinetics -A theoretical study. *Catalysis Communications*, January 2008.
- [10]. Lin Y. H and Leu J. Y (2008): Kinetics of reactive azo-dye decolorization by *Pseudomonas luteola* in a biological activated carbon process. *Biochemical Engineering Journal* 39:457–467
- [11]. Nwankwo, N. and Ifeadi, C.N. (1988), "Case Studies on the Environmental Impact of Oil Production and Marketing in Nigeria", University of Lagos, Nigeria.

- [12]. Speitel G. E Jr, Asce M, Dovantzis K, Digiano F. A (1987): Mathematical modelling of bioregeneration in GAC columns. Journal of Environmental Engineering 113(1):32-48
- [13]. Ullhyan, A & Ghosh, U. K (2012): Biodegradation of Phenol with Immobilised Pseudomonas Putida Activated Carbon Packed Bio-Filter Tower. Published in the African Journal of Biotechnology. Vol. 11 (85), pp. 15160 - 15167. October 2012.
- [14]. Walker, G. M & Weatherley, L. R (1997): A simplified predictive model for biologically activated carbon fixed beds. Process Biochemistry. 32 (4):327-335

APPENDIX

Table I: Model simulation at 10ml of bacteria

S/No	Days	t	CAO	CA	r_A	R	CA ²	R.CA	r_m
1	4	24	25.48	23.93	0.064583	370.529	572.6449	8866.76	0.077582
2	5	48	25.48	23.701	0.037063	639.4874	561.7374	15156.49	0.043619
3	6	72	25.48	23.462	0.028028	837.0981	550.4654	19640	0.029753
4	7	96	25.48	23.255	0.023177	1003.362	540.795	23333.18	0.023234
5	8	120	25.48	22.794	0.022383	1018.347	519.5664	23212.2	0.015466
6	9	144	25.48	22.749	0.018965	1199.508	517.517	27287.6	0.014967
7	10	168	25.48	22.708	0.0165	1376.242	515.6533	31251.71	0.014537
8	11	192	25.48	22.645	0.014766	1533.63	512.796	34729.04	0.013921
9	12	216	25.48	22.617	0.013255	1706.347	511.5287	38592.45	0.013663
10	13	240	25.48	22.585	0.012063	1872.332	510.0822	42286.61	0.013378
11	14	264	25.48	22.5	0.011288	1993.289	506.25	44848.99	0.012673
12	15	288	25.48	22.466	0.010465	2146.718	504.7212	48228.17	0.01241
13	16	312	25.48	20.771	0.015093	1376.206	431.4344	28585.17	0.018499
14	17	336	25.48	18.708	0.020155	928.2174	349.9893	17365.09	0.019457
15	18	360	25.48	16.931	0.023747	712.9676	286.6588	12071.25	0.020583
16	19	384	25.48	15.884	0.02499	635.6248	252.3015	10096.27	0.021444
17	20	408	25.48	14.93	0.025858	577.3877	222.9049	8620.398	0.022414
18	21	432	25.48	13.533	0.027655	489.3493	183.1421	6622.364	0.024301
19	22	456	25.48	11.22	0.031272	358.7882	125.8884	4025.604	0.029838
20	23	480	25.48	9.781	0.032706	299.056	95.66796	2925.067	0.037117
21	24	504	25.48	7.308	0.036056	202.6872	53.40686	1481.238	0.10416

Table II: Model simulation at 20ml of bacteria

S/No	t	CAO	CA	r_A	R	CA ²	R.CA	r_m
1	4	24	25.48	23.88	0.066667	358.2	8553.816	0.049851519
2	5	48	25.48	23.82	0.034583	688.7711	16406.53	0.045902372
3	6	72	25.48	23.51	0.027361	859.2487	20200.94	0.032422989
4	7	96	25.48	23.07	0.025104	918.971	21200.66	0.022667899
5	8	120	25.48	22.82	0.022167	1029.474	23492.59	0.019273498
6	9	144	25.48	22.4	0.021389	1047.273	23458.91	0.01530741
7	10	168	25.48	22.366	0.018536	1206.644	26987.79	0.015051586
8	11	192	25.48	22.358	0.01626	1374.996	30742.15	0.014992519
9	12	216	25.48	22.357	0.014458	1546.305	34570.75	0.014985166
10	13	240	25.48	22.346	0.013058	1711.244	38239.47	0.014904706
11	14	264	25.48	22.341	0.01189	1878.95	41977.62	0.014868392
12	15	288	25.48	22.1	0.011736	1883.077	41616	0.01329029
13	16	312	25.48	19.886	0.017929	1109.123	22056.01	0.022392794
14	17	336	25.48	17.237	0.024533	702.6122	12110.93	0.023047841
15	18	360	25.48	16.944	0.023711	714.6017	12108.21	0.023135696
16	19	384	25.48	14.188	0.029406	482.4825	6845.461	0.02418938
17	20	408	25.48	11.894	0.033299	357.1877	4248.39	0.025570292
18	21	432	25.48	9.629	0.036692	262.4269	2526.908	0.027886339

19	22	456	25.48	6.535	0.041546	157.2953	42.70623	1027.925	0.035991126
20	23	480	25.48	3.358	0.046088	72.8614	11.27616	244.6686	0.249507322
21	24	504	25.48	1.988	0.046611	42.65077	3.952144	84.78974	-0.03367417

Table III: Model simulation at 30ml of bacteria

S/No	t	CAO	CA	r_A	R	CA ²	R.CA	r_m	
1	4	24	25.48	22.914	0.106917	214.3164	525.0514	4910.847	0.095968
2	5	48	25.48	22.401	0.064146	349.2199	501.8048	7822.874	0.062206
3	6	72	25.48	21.987	0.048514	453.2104	483.4282	9964.738	0.048003
4	7	96	25.48	21.533	0.041115	523.7314	463.6701	11277.51	0.038083
5	8	120	25.48	21.188	0.035767	592.3952	448.9313	12551.67	0.032747
6	9	144	25.48	21.11	0.030347	695.6156	445.6321	14684.44	0.031722
7	10	168	25.48	21.102	0.02606	809.7615	445.2944	17087.59	0.03162
8	11	192	25.48	20.668	0.025063	824.6584	427.1662	17044.04	0.026841
9	12	216	25.48	20.183	0.024523	823.0183	407.3535	16610.98	0.022812
10	13	240	25.48	20.112	0.022367	899.1952	404.4925	18084.61	0.022309
11	14	264	25.48	20.011	0.020716	965.9726	400.4401	19330.08	0.021624
12	15	288	25.48	19.6	0.020417	960	384.16	18816	0.019166
13	16	312	25.48	16.981	0.02724	623.3759	288.3544	10585.55	0.032033
14	17	336	25.48	13.66	0.035179	388.3046	186.5956	5304.24	0.032658
15	18	360	25.48	10.814	0.040739	265.4466	116.9426	2870.54	0.033539
16	19	384	25.48	7.716	0.04626	166.7949	59.53666	1286.989	0.035378
17	20	408	25.48	5.842	0.048132	121.3737	34.12896	709.0649	0.037692
18	21	432	25.48	3.77	0.050255	75.01796	14.2129	282.8177	0.044239
19	22	456	25.48	1.077	0.053515	20.12507	1.159929	21.6747	-0.19693
20	23	480	25.48	0.933	0.05114	18.24418	0.870489	17.02182	-0.09042
21	24	504	25.48	0.526	0.049512	10.62371	0.276676	5.58807	-0.02189

Table IV: Model simulation at 40ml of bacteria

S/No	t	CAO	CA	r_A	R	CA ²	R.CA	r_m	
1	4	24	25.48	22.271	0.133708	166.564	495.9974	3709.548	0.116643
2	5	48	25.48	21.508	0.08275	259.9154	462.5941	5590.261	0.086599
3	6	72	25.48	20.333	0.071486	284.4329	413.4309	5783.374	0.060371
4	7	96	25.48	20.164	0.055375	364.1354	406.5869	7342.427	0.05769
5	8	120	25.48	19.897	0.046525	427.6625	395.8906	8509.202	0.053831
6	9	144	25.48	19.016	0.044889	423.6238	361.6083	8055.629	0.043622
7	10	168	25.48	19	0.038571	492.5926	361	9359.259	0.043465
8	11	192	25.48	18.133	0.038266	473.8718	328.8057	8592.717	0.036094
9	12	216	25.48	17.674	0.036139	489.0576	312.3703	8643.605	0.032916
10	13	240	25.48	17.611	0.032788	537.1254	310.1473	9459.316	0.032512
11	14	264	25.48	17.489	0.030269	577.787	305.8651	10104.92	0.031748
12	15	288	25.48	17.066	0.029215	584.1464	291.2484	9969.043	0.029288
13	16	312	25.48	14.591	0.034901	418.0726	212.8973	6100.097	0.038516
14	17	336	25.48	11.796	0.040726	289.6416	139.1456	3416.613	0.038961
15	18	360	25.48	8.844	0.046211	191.3825	78.21634	1692.587	0.03976
16	19	384	25.48	5.533	0.051945	106.5159	30.61409	589.3523	0.041813
17	20	408	25.48	2.994	0.055113	54.325	8.964036	162.6491	0.047348
18	21	432	25.48	1.877	0.054637	34.35428	3.523129	64.48298	0.057162
19	22	456	25.48	1.087	0.053493	20.32026	1.181569	22.08812	0.095872
20	23	480	25.48	0.621	0.05179	11.99083	0.385641	7.446304	-0.46229
21	24	504	25.48	0.339	0.049883	6.795911	0.114921	2.303814	-0.03759

Table V: Model simulation at 25°C temperature

S/No	t	CAO	CA	r_A	R	CA ²	R.CA	r_m	
1	4	24	24.349	20.188	0.173375	116.4412	407.5553	2350.716	0.088682
2	5	48	24.349	18.835	0.114875	163.9608	354.7572	3088.202	0.086868
3	6	72	24.349	18.196	0.085458	212.9225	331.0944	3874.337	0.085947
4	7	96	24.349	17.886	0.067323	265.6748	319.909	4751.859	0.085485
5	8	120	24.349	17.513	0.056967	307.4254	306.7052	5383.941	0.084913
6	9	144	24.349	15.159	0.063819	237.5295	229.7953	3600.71	0.080884
7	10	168	24.349	12.228	0.072149	169.483	149.524	2072.439	0.074574
8	11	192	24.349	9.741	0.076083	128.0307	94.88708	1247.147	0.06761
9	12	216	24.349	9.212	0.070079	131.4522	84.86094	1210.938	0.065873
10	13	240	24.349	8.884	0.064438	137.87	78.92546	1224.837	0.064742
11	14	264	24.349	7.808	0.062655	124.6183	60.96486	973.02	0.060709
12	15	288	24.349	5.791	0.064438	89.87003	33.53568	520.4373	0.051485
13	16	312	24.349	4.664	0.063093	73.92268	21.7529	344.7754	0.062153
14	17	336	24.349	3.99	0.060592	65.84999	15.9201	262.7415	0.061321
15	18	360	24.349	2.83	0.059775	47.34421	8.0089	133.9841	0.059078
16	19	384	24.349	2.526	0.056831	44.44778	6.380676	112.2751	0.058197
17	20	408	24.349	1.944	0.054914	35.40067	3.779136	68.8189	0.055875
18	21	432	24.349	1.606	0.052646	30.50574	2.579236	48.99222	0.053909
19	22	456	24.349	1.207	0.05075	23.78325	1.456849	28.70638	0.050531
20	23	480	24.349	0.962	0.048723	19.7443	0.925444	18.99402	0.04748
21	24	504	24.349	0.785	0.046754	16.79002	0.616225	13.18016	0.044496

Table VI: Model simulation at 27°C temperature

S/No	t	CAO	CA	r_A	R	CA ²	R.CA	r_m	
1	4	24	24.349	24.344	0.000208	116851.2	592.6303	2844626	0.000212517
2	5	48	24.349	24.338	0.000229	106202.2	592.3382	2584749	0.000219643
3	6	72	24.349	24.334	0.000208	116803.2	592.1436	2842289	0.000224668
4	7	96	24.349	24.214	0.001406	17218.84	586.3178	416937.1	0.000724304
5	8	120	24.349	24.166	0.001525	15846.56	583.9956	382947.9	0.006946913
6	9	144	24.349	22.616	0.012035	1879.229	511.4835	42500.64	0.022803575
7	10	168	24.349	18.98	0.031958	593.8983	360.2404	11272.19	0.023524794
8	11	192	24.349	16.841	0.039104	430.6702	283.6193	7252.917	0.024127651
9	12	216	24.349	15.002	0.043273	346.6815	225.06	5200.916	0.02481948
10	13	240	24.349	13.629	0.044667	305.1269	185.7496	4158.574	0.025493871
11	14	264	24.349	12.254	0.045814	267.4705	150.1605	3277.584	0.026372435
12	15	288	24.349	11.06	0.046142	239.693	122.3236	2651.004	0.02738219
13	16	312	24.349	8.361	0.051244	163.1619	69.90632	1364.196	0.031360169
14	17	336	24.349	6.574	0.052902	124.268	43.21748	816.9379	0.037414752
15	18	360	24.349	5.08	0.053525	94.90892	25.8064	482.1373	0.050950186
16	19	384	24.349	3.208	0.055055	58.26933	10.29126	186.928	0.7168351
17	20	408	24.349	2.894	0.052586	55.03388	8.375236	159.2681	-0.251691983
18	21	432	24.349	1.979	0.051782	38.21761	3.916441	75.63266	-0.034094298
19	22	456	24.349	1.526	0.05005	30.48924	2.328676	46.52659	-0.018818751
20	23	480	24.349	0.88	0.048894	17.99821	0.7744	15.83843	-0.007722562
21	24	504	24.349	0.599	0.047123	12.71141	0.358801	7.614135	-0.004670693

Table VII: Model simulation at 35°C temperature

S/No	t	CAO	CA	r_A	R	CA ²	R.CA	r_m	
1	4	24	24.349	20.934	0.142292	147.1204	438.2324	3079.817	0.06038
2	5	48	24.349	19.88	0.093104	213.5243	395.2144	4244.863	0.060113
3	6	72	24.349	19.839	0.062639	316.7202	393.5859	6283.412	0.060102
4	7	96	24.349	19.274	0.052865	364.5919	371.4871	7027.145	0.059948
5	8	120	24.349	19.175	0.043117	444.7236	367.6806	8527.575	0.05992
6	9	144	24.349	17.8	0.045479	391.388	316.84	6966.706	0.059503
7	10	168	24.349	15.734	0.05128	306.8267	247.5588	4827.611	0.058755
8	11	192	24.349	13.99	0.053953	259.2992	195.7201	3627.595	0.057972
9	12	216	24.349	13.4	0.05069	264.3529	179.56	3542.329	0.057667
10	13	240	24.349	12.656	0.048721	259.7657	160.1743	3287.594	0.057247
11	14	264	24.349	11.172	0.049913	223.83	124.8136	2500.629	0.056267
12	15	288	24.349	9.534	0.051441	185.3386	90.89716	1767.019	0.054889
13	16	312	24.349	7.877	0.052795	149.2001	62.04713	1175.249	0.053027
14	17	336	24.349	6.69	0.052557	127.2915	44.7561	851.5799	0.051251
15	18	360	24.349	5.88	0.051303	114.6137	34.5744	673.9284	0.049729
16	19	384	24.349	4.109	0.052708	77.95731	16.88388	320.3266	0.044974
17	20	408	24.349	3.77	0.050439	74.74416	14.2129	281.7855	0.043726
18	21	432	24.349	3.502	0.048257	72.56987	12.264	254.1397	0.042629
19	22	456	24.349	2.183	0.04861	44.90878	4.765489	98.03587	0.035134
20	23	480	24.349	1.774	0.047031	37.7196	3.147076	66.91457	0.03172
21	24	504	24.349	1.535	0.045266	33.91076	2.356225	52.05301	0.02935

Table VIII: Model simulation at 40°C temperature

S/No	t	CAO	CA	r_A	R	CA ²	R.CA	r_m	
1	4	24	24.349	21.192	0.131542	161.1048	449.1009	3414.134	0.038093
2	5	48	24.349	21.161	0.066417	318.6098	447.7879	6742.102	0.060434
3	6	72	24.349	21.097	0.045167	467.0923	445.0834	9854.245	0.060419
4	7	96	24.349	20.764	0.037344	556.0234	431.1437	11545.27	0.060338
5	8	120	24.349	20.685	0.030533	677.4563	427.8692	14013.18	0.060319
6	9	144	24.349	19.511	0.033597	580.7325	380.6791	11330.67	0.060013
7	10	168	24.349	18.813	0.032952	570.9147	353.929	10740.62	0.059815
8	11	192	24.349	18.29	0.031557	579.5808	334.5241	10600.53	0.059658
9	12	216	24.349	17.893	0.029889	598.6506	320.1594	10711.65	0.059533
10	13	240	24.349	17.147	0.030008	571.4079	294.0196	9797.932	0.059284
11	14	264	24.349	16.64	0.029201	569.8482	276.8896	9482.275	0.059104
12	15	288	24.349	16.116	0.028587	563.7566	259.7255	9085.501	0.058906
13	16	312	24.349	14.292	0.032234	443.3831	204.2613	6336.831	0.05812
14	17	336	24.349	11.453	0.038381	298.4032	131.1712	3417.612	0.056469
15	18	360	24.349	11.056	0.036925	299.4177	122.2351	3310.363	0.056181
16	19	384	24.349	9.248	0.039326	235.1654	85.5255	2174.809	0.054607
17	20	408	24.349	8.724	0.038297	227.8011	76.10818	1987.337	0.054051
18	21	432	24.349	8.502	0.036683	231.7703	72.284	1970.511	0.053799
19	22	456	24.349	6.139	0.039934	153.7278	37.68732	943.7352	0.050249
20	23	480	24.349	2.982	0.044515	66.98928	8.892324	199.762	0.040156
21	24	504	24.349	2.252	0.043843	51.3648	5.071504	115.6735	0.035644

Table IX: Model simulation at 45°C temperature

S/No	t	CAO	CA	r_A	R	CA ²	R.CA	r_m	
1	4	24	24.349	23.81	0.022458	1060.186	566.9161	25243.02	0.021008
2	5	48	24.349	23.572	0.016188	1456.185	555.6392	34325.2	0.014567
3	6	72	24.349	23.54	0.011236	2095.031	554.1316	49317.03	0.013984
4	7	96	24.349	23.159	0.012396	1868.289	536.3393	43267.71	0.009417
5	8	120	24.349	23.128	0.010175	2273.022	534.9044	52570.46	0.009169
6	9	144	24.349	23.017	0.00925	2488.324	529.7823	57273.76	0.008374
7	10	168	24.349	22.953	0.00831	2762.252	526.8402	63401.97	0.007973
8	11	192	24.349	22.906	0.007516	3047.784	524.6848	69812.54	0.007701
9	12	216	24.349	22.874	0.006829	3349.684	523.2199	76620.67	0.007525
10	13	240	24.349	22.842	0.006279	3637.744	521.757	83093.35	0.007357
11	14	264	24.349	22.81	0.00583	3912.827	520.2961	89251.57	0.007195
12	15	288	24.349	22.43	0.006663	3366.253	503.1049	75505.06	0.005687
13	16	312	24.349	14.879	0.030353	490.2057	221.3846	7293.771	0.031669
14	17	336	24.349	13.674	0.031771	430.3948	186.9783	5885.218	0.031926
15	18	360	24.349	13.325	0.030622	435.1415	177.5556	5798.261	0.03201
16	19	384	24.349	10.485	0.036104	290.4097	109.9352	3044.946	0.032929
17	20	408	24.349	9.66	0.036002	268.3151	93.3156	2591.924	0.033313
18	21	432	24.349	9.47	0.034442	274.954	89.6809	2603.814	0.033412
19	22	456	24.349	5.251	0.041882	125.3773	27.573	658.3563	0.038038
20	23	480	24.349	2.57	0.045373	56.64172	6.6049	145.5692	0.056289
21	24	504	24.349	2.062	0.04422	46.63023	4.251844	96.15154	0.073246